Ab Initio Molecular Orbital Calculations of Electronic Couplings in the LH2 Bacterial Light-Harvesting Complex of *Rps. Acidophila*

Gregory D. Scholes, Ian R. Gould,[†] Richard J. Cogdell,[‡] and Graham R. Fleming*

Department of Chemistry, University of California, Berkeley, and Physical Biosciences Division, Lawrence Berkeley National Laboratory, Berkeley, California 94720-1460

Received: October 6, 1998; In Final Form: January 20, 1999

The results of ab initio molecular orbital calculations of excited states and electronic couplings (for energy transfer) between the B800 and B850 bacteriochlorophyll *a* (Bchl) chromophores in the peripheral light-harvesting complex (LH2) of the purple photosynthetic bacterium *Rhodopseudomonas acidophila* are reported. Electronic couplings are estimated from "supermolecule" calculations of Bchl dimers using the CI-singles methodology and 3-21G* or 6-31G* basis sets. A scheme for dissecting the coupling into contributions from the Coulombic coupling and the short-range coupling (i.e., dependent on interchromophore orbital overlap) is reported. B850 couplings are calculated to be [total (Coulombic + short)]: intrapolypeptide dimer 320 (265 + 55) cm^{-1} and interpolypeptide dimer 255 (195 + 60) cm^{-1} at the CIS/6-31G* level. These results differ significantly from those estimated using the point dipole approximation. The effect of including Mg ligands (His residues) and H-bonding residues (Trp and Tyr) is also investigated. The consequences for superradiance and energy transfer dynamics and mechanism are discussed.

1. Introduction

The antenna complexes of photosynthetic organisms play an important role in optimizing the efficacy of the conversion of incident radiation to usable energy resources. The arrangement of a dozen or more pigments in close mutual proximity is typical,[1−4] thereby achieving a high spatial and spectral absorption cross section for the associated reaction centers.[5−7] The proper functioning of such a system relies also on efficient energy migration to and among subsequent pigment−protein complexes en route to the primary donor of the reaction center. Extensive studies of the time scales involved have been reported.[7−17] It is the closely interacting arrangement of the cofactors which lies at the heart of much of the current uncertainty regarding the details of the mechanism of energy transfer in the various antenna systems of purple bacteria, cyanobacteria, and green plants. A key factor underlying these issues is the magnitude of the electronic coupling. In the present work we report the results of ab initio studies of electronic couplings for the LH2 complex of the purple photosynthetic bacterium *Rhodopseudomonas acidophila*.

Recently, structures of the peripheral light-harvesting complex (*sc.* LH2) of purple photosynthetic bacteria have been resolved.[1,4,18] These reveal that the structure is composed of units which consist of two transmembrane polypeptides (α and *β*) and associated pigments: a pair of closely interacting (ca. 4 Å closest approach) bacteriochlorophyll *a* (Bchl a) molecules (B850), oriented with their planes normal to the membrane surface; one Bchl a (B800) separated from the B850 pair by 18 Å and coplanar with the membrane surface; and one (possibly two) carotenoids (Car) which make close contact with the B800 and one of the B850 chromophores. Such a protamer unit and its relationship to its neighbor is depicted in Figure 1. The protamers are arranged in a highly symmetrical ring motif, found to have C_9 symmetry in *Rhodopseudomonas* (*Rps.*) *acidophila* and *Rhodovulum* (*Rhv.*) *sulfidophilum*, and C_8 symmetry in *Rhodospirillum* (*Rs.*) *molischianum*.

Clearly, much stronger interactions are expected between the B850 molecules than the B800s. Indeed, there has been much debate on the extent to which the electronic excited states of B850 are delocalized over neighboring molecules.[12−17,19−23] In order to understand such a system one needs information on the electronic coupling between molecules, the disorder, the coupling to the protein, the time scales of protein relaxation and of energy transfer. All except the couplings can be obtained from femtosecond nonlinear spectroscopy. However, to interpret properly the spectroscopy, the nature and magnitude of the electronic couplings must be understood. This is made clear in the recent work of Mukamel and co-workers.[24]

The LH2 structure data suggests that the basic building block of the antenna is the (protamer) α*β*-subunit, such that the B850 ring is composed of Bchl *a* molecules organized as dimers.[1,18] Accordingly, we will refer to the pair of Bchls within the subunit as intrapolypeptide, and a pair of Bchls from adjacent subunits as interpolypeptide.

Empirical calculations of the interactions and spectroscopy of the Bchl *a* pigments in LH2 from *Rps. acidophila*[25,26] and *Rs. molischianum*[27,28] have been reported recently. Sauer et al.[25] have improved upon the dipole−dipole model by using a point monopole approximation for each transition density. They concluded that the intra- and interpolypeptide couplings of *Rps. acidophila* are of a similar magnitude (291 and 271 cm^{-1} respectively), and asserted that excitation energy was delocalized over the entire B850 ring. Alden et al.[26] employed the QCFF/PI method and also concluded that the excited states of B850 are extensively delocalized. They determined the couplings to be 394 and 317 cm^{-1}, respectively (in the absence of dielectric screening), and found the orbital overlap-dependent contribution

[†] Department of Chemistry, Imperial College of Science, Technology and Medicine, London SW7 2AY, United Kingdom.
[‡] Division of Biochemistry and Molecular Biology, University of Glasgow, Glasgow G12 8QQ, United Kingdom.

10.1021/jp9839753 CCC: $18.00
Published on Web 03/12/1999

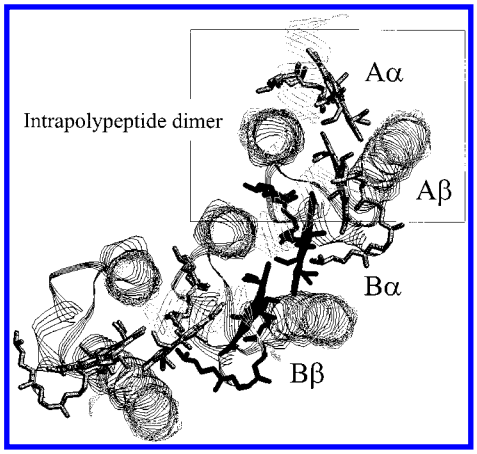

Figure 1. Illustration of a section of the B850 ring. Protein α helices are drawn as ribbons, and Bchls *a* are labeled according to the scheme of ref 29.

to the coupling to be small. They also examined the effect of dielectric screening, which was found to reduce the calculated couplings to 254 and 209 cm^{-1} for $n^2 = 2.0$. Hu et al.[27] used a combination of INDO/S/CI calculations (for the site energies) and spectral modeling to estimate the couplings in *Rs. molischianum*. Although the dipole approximation was not introduced, no account was made for spectral shifts induced by, for example, orbital overlap-dependent interactions. They determined couplings for this different species, one of which is much larger than obtained in the other studies (and in our work), 806 and 277 cm^{-1}. Again it was concluded that the spectroscopy is dominated by delocalization. It seems unlikely that this large difference arises from the structural differences between *Rs. molischianum* and *Rps. acidophila*, and probably relates to the method of calculation. In each of these studies the entire LH2 ring was considered. In the present work we calculate couplings between various chromophores in the ring; the exciton states of the ring may then be determined from these couplings. It should be noted here that experimental studies of superradiance, energy transfer dynamics in B850, and energy gap correlation functions (line broadening functions) suggest that excitation energy is delocalized over just two to four molecules.[7,8,10−17] The "delocalization length" depends on the experiment used to measure it, owing to its intimate entanglement with the density matrix. It depends on the excitation conditions, observation method, and time. In the present work, where we refer to "delocalization length", we mean the number of Bchl molecules over which excitation is delocalized on the time scale of energy migration.

The structure of LH2 is known, but there remain questions concerning the ramifications for electronic couplings. It is expected that the dipole approximation is inappropriate, given the close proximity of the chromophores—but how far in error is it? In ref 1 it was postulated that couplings which depend on interchromophore orbital overlap (short-range couplings) may by significant for B850—can this be quantified? Finally, what is the role of the H-bonding residues and Mg ligands? It is known that these interactions contribute significantly to the spectral shifts. Are there implications for the couplings? We address these issues quantitatively in the present work.

We investigate the relationship between structure and function by examining various pigment−pigment and pigment−protein interactions in the supramolecular assembly. Recently, we have described a method for accurately calculating Coulombic couplings between chromophores using transition densities, determined ab initio, which is valid at all separations.[29] We have applied this method to determine couplings between Car and Bchl *a* pigments in LH2. In the present work, we report the results of detailed calculations of the couplings (both Coulombic and those dependent on orbital overlap) between the B850 and between the B800 molecules.

There are three pertinent and, as yet unresolved, questions regarding the mechanism of energy migration in photosynthetic antenna systems: (i) To what degree are the initial absorbing states delocalized? (ii) Is energy transfer a hopping (Markovian) process, or a coherent exciton migration? (iii) Are energetic "funnels" a necessity in all or any antenna systems? Nonlinear spectroscopy can elucidate a crucial input parameter for any model of energy migration in a multichromophoric system (which is not necessarily in the very weak coupling limit) since it provides details of the electronic energy gap correlation function (i.e., the inhomogeneous and homogeneous line broadening).[13,19,20] Another crucial input requirement is the electronic couplings, the details of which are the subject of the present work.

2. Theory of Couplings

In the absence of direct interchromophore orbital overlap, two chromophores (one in an excited electronic state) interact via the long-range Coulombic mechanism.[29−33] Physically, the interaction involves deexcitation of the excited molecule together with a simultaneous excitation of the acceptor chromophore This interaction is mediated by an interaction between the transition moments of the two molecules and dominates the coupling in many instances of singlet−singlet energy transfer. The Coulombic potential may be represented as a multipolar expansion of the interaction potential and it is usual to retain only the dipole−dipole term (hence the signature R^{-3} distance dependence).

When the electron density distributions (i.e., orbitals) on the two chromophores overlap, additional effects arise (as a consequence of the Pauli principle) which can dramatically increase the electronic coupling.[32,34−36] Such a mechanism for energy transfer between forbidden transitions was first described by Dexter.[36] Broadly speaking, it is correct to attribute the primary overlap-dependent interactions to exchange "corrections"; however, it has been shown that by defining appropriate reactant and product states the coupling at close separations (or for forbidden transitions) is promoted primarily by terms other than the Dexter two-electron, four-center exchange integral.[34] However, the exponential distance dependence for the interaction is analogous to that introduced by Dexter (because the orbital overlap dependence is the same).[35] The detailed elucidation of the mechanism of this coupling is not merely a matter of semantics; it serves to establish a connection with charge transfer configurations, and hence implications for spectral shifts, hyperchromism and hypsochromism, superradiance, and polarizabilities of molecular aggregates.[37−40]

Recently, expressions for the electronic coupling have been developed using the framework of localized molecular orbitals (LMOs). Such a formalism explicitly involves charge transfer configurations, which have been found to play a central role in promoting those interactions which depend on orbital overlap.[34,35,41−44] To clarify the meaning of "charge transfer configurations", and to put the LMO theory into a more general perspective, we briefly expound here a formulation in terms of electron densities.

Following McWeeny,[45] we assume that each molecule in the aggregate is recognizably distinct: composed of groups of electrons $n_A(\Phi_A)$, $n_B(\Phi_B)$, etc. Then a symmetry-adapted

generalized product function corresponding to a particular assignment of states to the various electron groups may be written,

$$\Phi_\kappa(\boldsymbol{x}_1,\boldsymbol{x}_2,...,\boldsymbol{x}_N) = N_\kappa \hat{A}[\Phi_a^A(\boldsymbol{x}_1,...,\boldsymbol{x}_{n_A})\Phi_b^B(\boldsymbol{x}_{n_A+1},...,\boldsymbol{x}_{n_A+n_B})] \quad (1)$$

such that the group function Φ_r^R describes group R in state r, and κ = Aa,Bb,.... We assume that each group is antisymmetrized via the partial antisymmetrizers $\hat{A}_R = (n_R)^{-1}\sum\zeta_P P$ (where P denotes an orbital permutation and ζ_P accounts for the associated parity: $+1$ for an even number of interchanges, -1 for an odd number), then

$$\hat{A} = \frac{n_A! n_B! ...}{n!}\sum\zeta_T T \quad (2)$$

accounts for the sum of transposes which exchange variables between different groups. If the group functions are strongly nonorthogonal, then we should furthermore normalize to unity at infinite separation. We denote this factor below as K.

After making some mild approximations, as detailed elsewhere,[45] we arrive at the following expression (for operator O) which forms the basis for calculating the electronic coupling in a strongly interacting dimer where we have made use of the

$$\langle\Phi_{ab'}^{AB}|O|\Phi_{a'b}^{AB}\rangle = K^2\langle\hat{A}[\Phi_a^A\Phi_{b'}^B]|O|\hat{A}[\Phi_{a'}^A\Phi_b^B]\rangle = \langle\Phi_a^A\Phi_{b'}^B|O[1 - \sum_{i,\tilde{r}}(i,\tilde{r}) + \sum_{i,j,\tilde{r},\tilde{s}}(i,\tilde{r})(j,\tilde{s}) - ...]|\Phi_{a'}^A\Phi_b^B\rangle \quad (3)$$

idempotency of $\hat{A}$ and indices i, j, ... pertain to the functions of group A, while $\tilde{r},\tilde{s},...$ [$\equiv(r + n_a),(s + n_a),...$] pertain to group B.

The $\Phi_{a'}^A\Phi_b^B$ and $\Phi_a^A\Phi_{b'}^B$ of eq 3 correspond to the ψ_1 and ψ_4 of ref 34. By admitting the single electron exchange term, eq 3 then yields the H_{14} (or T_{14}) of Harcourt et al.[34] This is seen clearly by writing the wave functions as Slater determinants:

$$^{1,3}H_{14} \approx \langle^{1,3}\Phi_a^A\Phi_{b'}^B|H(1 - \sum_{i,\tilde{r}}(i,\tilde{r}))|^{1,3}\Phi_{a'}^A\Phi_b^B\rangle = \langle 2^{-1/2}(|(\text{core})ab\bar{a}\bar{b}'| \pm |(\text{core})ab'\bar{a}\bar{b}|)|\hat{H}|2^{-1/2}(|(\text{core})ab\bar{a}'\bar{b}| \pm |(\text{core})a'b\bar{a}\bar{b}|)\rangle \cong \langle(\text{core})ab\bar{a}\bar{b}'|H|(\text{core})(ab\bar{a}'b - ba'\bar{a}b - ab\bar{b}\bar{a}') \pm (\text{core})(a'b\bar{a}\bar{b} - ba'\bar{a}\bar{b} - a'b\bar{b}\bar{a})\rangle \quad (4)$$

where (core) denotes the core electrons. For clarity, we consider explicitly an active space of four orbitals (a, a', b, b') and the exchange of only four electrons. The group operator (containing intergroup exchange information) is written $\hat{H}$. $H = 1$ for an overlap matrix element or $H = \sum_\mu h(\mu) + \sum_{\mu<\nu} r_{\mu\nu}^{-1}$ for a Hamiltonian matrix element (in atomic units), with $h(\mu) \equiv {}^1/_2\nabla^2(\mu) - \sum_n Z_n/r_{n\mu}$ denoting the usual one-electron Hamiltonian operator, for electrons μ and ν and atomic centers n with charge Z_n.

As shown by Harcourt et al.,[34] additional configurations (those invoking intergroup charge transfer, ψ_2 and ψ_3) must be added to define properly the initial and final states such that electron exchange is properly included. This could be done by admitting intergroup single excitation configuration interaction. However, if the group functions have been determined variationally with the operator $\hat{H}$ (indeed, in the supermolecule SCF method, all orders of intergroup electron exchange have been treated variationally to obtain the wave functions), then the charge transfer configurations are implicitly accounted for via the group function analogue of Brillouin's theorem. In other words, the charge density cannot be improved further by single excitations because the polarization of each group in the presence of the others has already been taken into account.

Thus, the charge transfer configurations introduced explicitly to the LMO-based theory appear in a natural manner in the generalized product function approach. They represent the delocalization of electrons from one group (chromophore) to another. This basic result forms the foundation upon which electron correlation may be added. The most important contribution arises from intragroup double-excitation terms, such as the ψ_{1^*} and ψ_{4^*} of ref 46. In that work it was demonstrated that inclusion of these contributions to the group functions has a significant effect on the Coulombic coupling (lowering it concomitantly with the dipole transition moment) and a more mild influence on the orbital overlap-dependent coupling (increasing it somewhat).

In the present work we use a supermolecule CIS calculation to determine the electronic coupling. Thus, in effect, all exchange terms of eq 3 are included in our calculations. We have demonstrated previously the relationship between canonical molecular orbital methods and those based on localized orbitals.[47]

3. Structures

The LH2 structure data suggests that the basic building block of the antenna is the (protamer) $\alpha\beta$-subunit, such that the B850 ring is composed of Bchl *a* molecules organized as dimers.[1,18] In fact, such an assembly was proposed even prior to the availability of high-resolution structure data.[6,48] Recent investigations of energy transfer in LH2 furthermore suggest that a description based on interacting Bchl *a* dimers (cf. ref 49) provides a reasonable description of the dynamics.[12] We refer to the B850 Bchls as α-B850 and β-B850 according to the α helix which contains the histidine residue coordinating to the central Mg of the Bchl; such that α is inside the LH2 ring and β is on the outside. This is depicted in Figure 1 (and see ref 29 for the labeling convention which we have adopted). The β-B850 is markedly distorted from planarity.

A low-resolution projection map of the core antenna complex LH1 of *Rps. rubrum* suggests that the structure has many similarities with that of LH2.[3] Thus, an understanding of the relationship between electronic couplings and structure of LH2 should provide many insights into the nature and function of LH1. The LH1 complex of *Rps. rubrum* may be dissociated (by addition of the detergent β-octylglucoside) into smaller complexes, B820.[50,51] These complexes (thought to be composed of dimeric Bchl *a*) may be further dissociated or reassociated.

Studies of the spectra and energy transfer of site-directed mutant strains of the LH2 of *Rb. sphaeroides* have suggested that the influence of the H-bonding residues αTyr44, αTyr45 (αTyr44, αTrp45 in *Rps. acidophila*) from the adjacent α protein to the C3-acetyl group of B850 Bchl *a* contributes significantly to the spectral shift (compared to B800 or to 777 nm in organic solvent).[52] This is supported by the X-ray crystal structure data of the B800−B850[53] and B800−B820[54] LH2 complexes of *Rps. acidophila*. In the B800−B820 complex αTyr44 and αTrp45 which H-bond to the ring I acetyl goups of the βB850 and αB850 Bchl are replaced by Phe and Leu, resulting in a complex which absorbs at 800 and 820 nm. To investigate what role the αTyr44 and αTrp45 residues may have in perturbing the coupling, we report here calculations of B850 dimer couplings in which we have taken account of these residues. However, we have not investigated specific structural changes

in the Bchl such as rotation of the ring I acetyl group out of the plane of the macrocycle as suggested by preliminary X-ray crystal structure data of the B800−B820 complex.[54]

It is also well-known that the central Mg of Bchl (or Chl) should be described by a coordination number of greater than 4; that is, the Mg is typically coordinated to a Lewis base. In the case of the B850 Bchls of LH2, the central Mg coordinates to a His ligand.[55] Thus we also include these ligands in the "H-bond" calculations.

Atomic coordinates used for the calculations were those from the 2.5 Å resolution crystal structure of *Rps. acidophila* (strain 10050) reported by McDermott et al.[1] α-B850$_A$ and β-B850$_B$ correspond to BCL P6 and BCL Q1, respectively. The B800$_B$ corresponds to BCL P9. We have also examined the B850 Bchls BCL P1 through BCL P4, specifically for examining the influence of H-bonding residues. Hydrogen atoms were added to X-ray structures using MNDO geometry optimization (keeping heavy atoms fixed).

4. Methods

CIS Calculations. We report HF MO densities and CI-singles results calculated using Gaussian 94.[56,57] We report calculations using both 3-21G* and 6-31G* basis sets.[58] The largest calculations involved 624 electrons and 1442 basis functions. A CIS orbital window was employed for the 6-31G* dimer calculations from the frozen core to orbital 938 (i.e., the same as the default for the 3-21G* calculations). Test calculations convinced us that use of the CI window has a negligible impact on the results.

Semiempirical methods have been shown to provide great utility for such calculations[59,60] and are parametrized such that experimental excitation energies are closely reproduced without needing to admit higher order CI (than CIS) to the calculation. When such methods are used, however, careful consideration must be given to the form of the orbital overlap integrals, especially their long-range behavior, because the primary contribution to the orbital overlap-dependent coupling is given by core integrals of the form $\beta_{\mu\nu} = -\beta^0 S_{\mu\nu}$, where β^0 is a parameter (for example, the ionization energy of a carbon 2p orbital).[61−63] In the INDO/S/CI method[62,64] the overlap integral is given by the formulas of Mulliken et al.,[65] assuming Slater-type atomic orbitals, with an exponent of 3.07 Å^{-1} (1.625 bohr^{-1}) and $\beta^0 = -21$ eV for C 2s and 2p. For the QCFF method[63] as employed by Alden et al.,[26] a parametrized biexponential function is used for intermolecular orbital overlaps, with exponents of 1.95 and 0.7 Å^{-1}. Previously, a Mulliken-based form with $\beta^0 = -10.5$ eV (the ionization potential of C) has also been investigated.[37,66,67] The distance dependence of these various empirical core integrals may be compared, and it is found that they are all quite similar (and exhibit the expected rapid attenuation with donor−acceptor separation).

We employ ab initio wave functions here so that a rigorous approach, amenable to systematic improvement can be developed. No approximations pertaining to integral evaluation are involved in an ab initio MO calculation, for which the orbital overlap contribution will usually be underestimated but may be improved systematically with basis set size. We reiterate that the calculations reported here are based on variationally determined ground state dimer wave functions, and thus include accurate account of the (in LMO language) charge transfer configurations, i.e., the intermolecular electron exchanges which mediate most of the short-range coupling. This circumvents the necessity of determining the energy gap between the locally excited and charge transfer configurations in the basis of monomer wave functions and orbitals.

In the present work the CIS coupling is not calculated directly, but is estimated from the CIS "supermolecule" calculations of the excited states. Thus we base our analysis on the premise that the CIS coupling is reliably represented in the calculated splitting of the dimer excitation energy. At the CIS level of theory this is a good approximation, but the influence of higher-order CI has not been clearly established.[37] Considering that excitation energies for each transition are overestimated by the CIS method (owing to neglect of electron correlation; especially $\sigma-\pi$ dynamic correlation[68]), this may at first be thought questionable. However, upon consideration of the symmetry (with respect to CI composition) of the CIS wave functions (i.e., the exciton states), which contrasts to that of the closed-shell ground state, it is reasonable to assume that even though the excitation energies are overestimated, the splitting between the dimer states should be reasonably well estimated. It is noted, however, that this is probably not the case for a dimer of high symmetry (e.g. the D_{2h} symmetry ethene dimer examined in ref 37).

We interpret the CIS results by recourse to the LMO basis set discussed previously. Thus we consider the localized configurations ψ_1 and ψ_4 and the charge transfer configurations ψ_2 and ψ_3. These latter configurations account for orbital overlap-dependent coupling, as discussed above, and contribute to the shifts of the dimer spectrum with respect to that of the monomers.[37,47] We account for the site disorder by writing $H_{44} = H_{11} + \Delta$, then, assuming that $H_{22} - H_{11}$, etc., $\gg \Delta$ and reducing the problem to an effective two-state problem, we need to solve the secular determinant of eq 5

$$\begin{vmatrix} -U - \epsilon_j & V^{\mathrm{CIS}} \\ V^{\mathrm{CIS}} & \Delta - U - \epsilon_j \end{vmatrix} = 0 \qquad (5)$$

where U is related to the short-range contribution to the coupling. Knowing the CIS excitation energies of each monomer (H_{11} and H_{44}) and the dimer CIS excitation energies (E_1 and E_2), we arrive at the working equations:

$$V^2 = \epsilon_j^2 + \epsilon_j(2U - \Delta) + U^2 - U\Delta$$

$$\epsilon_1^2 - \epsilon_2^2 + (\epsilon_1 - \epsilon_2)(2U - \Delta) = 0 \qquad (6)$$

where $\epsilon_j = E_j - H_{11}$.

We have found the resultant coupling to be reasonably precise, but it bears poor relationship to experiment owing mainly to the overestimated Coulombic coupling (ca. a factor of 4). To remedy this, we have attempted to dissect the coupling into contributions from the Coulombic coupling (which we then rescale as discussed below) and the short-range (i.e., orbital overlap-dependent) coupling (which we take as a reasonable zero-order estimate). There are a number of approximations involved in this analysis of the CIS calculations which we discuss below.

Determination of the Coulombic Coupling. For the case of allowed singlet transitions, the dominant contribution to the electronic coupling arises from the resonance, or Coulombic, coupling, as described by Förster (in the dipole approximation). In terms of the transitions densities between the relevant electronic states of the group functions corresponding to donor and acceptor, we may write this Coulombic coupling exactly as in eq 7

$$V_{a'b}^{AB}(\mathrm{Coul}) = \frac{e^2}{4\pi\epsilon_0}\int\frac{P_A(aa'|\boldsymbol{r}_1)P_B(b'b|\boldsymbol{r}_2)}{r_{12}}\,\mathrm{d}\boldsymbol{r}_1\,\mathrm{d}\boldsymbol{r}_2 \quad (7)$$

where, following McWeeny,[45] the transition density connecting pairs of states Ψ_K and Ψ_L is given by eq 8,

$$\rho(KL|\boldsymbol{x}_1;\boldsymbol{x}_1') = N\int\Psi_K(\boldsymbol{x}_1,\boldsymbol{x}_2,...,\boldsymbol{x}_N)\Psi_L^*(\boldsymbol{x}'_1,\boldsymbol{x}'_2,...,\boldsymbol{x}'_N)\,\mathrm{d}\boldsymbol{x}_2\ldots\mathrm{d}\boldsymbol{x}_N\,\mathrm{d}\boldsymbol{x}'_2\ldots\mathrm{d}\boldsymbol{x}'_N \quad (8)$$

and when dealing with spinless operators (such as r^{-1}) we may integrate over spin,

$$P(KL|\boldsymbol{r}_1) = \int\rho(KL|\boldsymbol{x}_1)\,\mathrm{d}s_1 \quad (9)$$

then we note that

$$\int P(KK|\boldsymbol{r}_1)\,\mathrm{d}\boldsymbol{r}_1 = N_{\mathrm{elec}} \quad (10a)$$

$$\int P(KL|\boldsymbol{r}_1)\,\mathrm{d}\boldsymbol{r}_1;\ K \neq L = 0 \quad (10b)$$

and the dipole transition moment is given by

$$\mu_\alpha^{LK} = \langle\Psi_L|\sum_i(r_\alpha)_i|\Psi_K\rangle = \int(r_\alpha)_1 P(KL|r_1)\,\mathrm{d}\boldsymbol{r}_1 \quad (11)$$

Krueger et al.[29] have recently described a method for the practical calculation of the Coulombic coupling of eq 7 using ab initio wave functions. This is done by calculating transition density cubes (TDCs) corresponding to eq 9, given by eq 12

$$\tilde{P}(KL|x,y,z) = V_\delta\int_z^{z+\delta_z}\int_y^{y+\delta_y}\int_x^{x+\delta_x}P(KL|\boldsymbol{r}_1) \quad (12)$$

where the δ_α denote the grid size of the transition density cube and $V_\delta = \delta_x\delta_y\delta_z$ is the element volume.

In the present work we calculate the Coulombic coupling, V^{Coul}, corresponding to the interaction between the CIS transition densites of molecules A and B. Thus the calculation of the Coulombic coupling is determined from ab initio wave functions for each of A and B. However, it is well-known that the CI-singles method significantly overestimates the magnitude of electronic transition moments, mainly owing to neglect of $\sigma-\pi$ dynamic correlation effects.[68] This means that if we simply take the "raw" Coulombic couplings, they are overestimated by a factor of about 4, so in order to put them into perspective with experiment we use an approximate scaling scheme. In order to do this we need to assume that the leading moment of the transition density (note: but not necessarily the coupling) is the dipole transition moment. Then it is reasonable to scale each of the transition density cubes by the ratio of experimental to CIS transition dipole moments: $|\mu^{\mathrm{exp}}|/|\mu^{\mathrm{CIS}}|$. We still have ab inito Coulombic couplings, we have simply rescaled their magnitudes to account for a well-characterized deficiency in the CIS calculation. On the other hand, the short-range interactions are not dependent on transition moments, and therefore should not be scaled in this manner. This is why we needed to adopt a fairly complicated scheme for the calculation of the total couplings.

There are two additional sources of error inherent in the TDC method. First, there are numerical errors associated with integrating the transition density into a finite volume, with finite cell size. Second, the monomer transition densities which we employ are determined from CIS calculations based on monomer HF reference determinants, and hence no account is taken of polarization of these reference wave functions by the presence of the other half of the dimer (ideally each monomer HF wave function would be determined variationally in the self-consistent reaction field of the other).

Overlaps and Normalization. To calculate the total coupling between the reactant and product wave functions (Ψ_R and Ψ_P) one should take the normalization factors (N_R and N_P in the language of ref 34) into account. It is generally assumed that these are small enough to be neglected to a good approximation. We shall demonstrate here that this is indeed the case for the dimers we study in this work.

The relationship between localized molecular orbitals (LMOs) and canonical molecular orbitals (CMOs) is developed in ref 47. Following from that work, and assuming $N_R \approx N_P = N$, we consider one of the dimer stationary states,

$$\Psi_{(-)} = C_1\Phi_1 + C_4\Phi_4 \cong N_{(-)}(\Psi_R - \Psi_P) \quad (13)$$

with $N_{(-)} \cong N/(2 - 2S_{RP})^{1/2} \approx N/\sqrt{2}$ for small overlap. Hence, $N^2 = 2(C_1K_1 + C_4K_4)^2$ where C_1 and C_4 are normalized coefficients from the CIS calculation. The K_1 and K_4 are expressed in terms of the overlaps of monomer orbitals, S_{ab} and $S_{a'b'}$. After evaluating these overlap integrals (see below) we find that $2N^2 \approx 0.99$; thus the normalization may be neglected even if the overlap integrals were an order of magnitude larger.

We evaluate the orbital overlap integrals from density matrices for the appropriate orbitals (a and b), which are first normalized according to $S_{aa} = S_{bb} = 1$, then

$$S_{ab} = (\int\int\int\rho_a(x,y,z)\rho_b(x,y,z)\,\mathrm{d}x\,\mathrm{d}y\,\mathrm{d}z)^{1/2} \quad (14)$$

Précis. To summarize, our approach for estimating electronic couplings from the CIS supermolecule calculations involves the following:

(i) calculate the excited states of the dimer;

(ii) calculate the excited states of each component monomer;

(iii) use (i) and (ii) with eqs 5 and 6 to give the CIS coupling, V^{CIS};

(iv) calculate transition densities for each monomer, then the CIS Coulombic coupling, $V^{\mathrm{Coul,CIS}}$, from eq 7 (using a scaling factor $|\mu_A^{\mathrm{CIS}}||\mu_B^{\mathrm{CIS}}|/|\mu_A^{\mathrm{cube}}||\mu_B^{\mathrm{cube}}|$, which is not quite unity owing to numerical errors associated with the cubes);

(v) determine the calculated short-range coupling, $V^{\mathrm{short}} = V^{\mathrm{CIS}} - V^{\mathrm{Coul,CIS}}$;

(vi) rescale $V^{\mathrm{Coul,CIS}}$ relative to the experimental transition moments, to give $V^{\mathrm{Coul}} = V^{\mathrm{Coul,\ CIS}} \times |\mu_A^{\mathrm{exp}}||\mu_B^{\mathrm{exp}}|/|\mu_A^{\mathrm{CIS}}||\mu_B^{\mathrm{CIS}}|$;

(vii) finally, we have the coupling $V = V^{\mathrm{short}} + V^{\mathrm{Coul}}$.

5. Results

It is evident from the analysis of the dimer calculations (see below) that results obtained using the 3-21G* and 6-31G* basis sets are very similar. Of course, the short-range couplings determined using the more flexible basis set are larger, but it is evident that the 3-21G* basis set provides results of sufficient accuracy for our investigation. In Table 1 the calculated transition moment directions (3-21G*) are specified relative to the internal atomic coordinates for the B850 molecules. It is seen that the transition moment vector lies very close to the Mg−N direction, as expected.

The results of the monomer calculations are summarized in Table 2. It is noted that the excitation energies and the transition moments are overestimated (as expected from a CIS calculation[68]); experimental values are ca. 1.60 eV and 1.33 e Å, respectively. Owing to its distorted structure, the excitation

TABLE 1: Transition Moment Direction for the Bchl a Q_y Transitions Relative to the Internal Coordinates from the Crystal Structure Data (in Å)[1]

	Mg	N_A	N_B	$\hat{\mu}$
αB850	(0,0,0)	(0,0,2.0557)	(2.0067,0,−0.0303)	(−0.9998, 0.024, 0.0007)
*β*B850	(0,0,0)	(0,0,2.0592)	(1.993,0,−0.0248)	(−0.9974, 0.0687, −0.0054)

TABLE 2: Summary of the Properties (Excitation Energy, Δ*E*, and Dipole Transition Moment, *μ*) Calculated for the Bchl *a* Monomers (Which Compose the Intrapolypeptide Dimer)[a]

monomer	Δ*E*, eV	|*μ*|, e Å	Δ*E*, nm
3-21G*			
α (1)	1.9214	2.073	645
β (6)	1.8795	2.048	660
B800	1.8927	2.017	655
α-His (3)	1.8955	2.040	654
β-His (2)	1.8629	2.031	666
α-H bond (3)	1.9031	2.088	651
β-H bond (2)	1.8786	2.040	660
6-31G*			
α (1)	1.7687	2.134	701
β (6)	1.7279	2.108	718

[a] The B850 molecules are denoted α and *β*; His denotes that the His Mg ligand is included in the calculation; H-bond denotes that the αTrp or αTyr, for α or *β*, respectively, are also included, α is planar, *β* is buckled.

TABLE 3: Summary of the Dimer Calculations: Excitation Energies (Δ*E*), Transition Moment Magnitudes (\|*μ*\|), *U* and V^{CIS} from Eqs 5 and 6, and the Orbital Overlap Integrals between HOMOs (upper) and LUMOs (lower)[a]

dimer	Δ*E*, eV	|*μ*|, e Å	*U*	V^{CIS}, eV	*S*
3-21G*					
$(A\alpha\text{-}A\beta)_{intra}$	1.8030	3.074	0.0085	0.0862	1.72E−3
	1.9803	0.635			−5.28E−3
$(A\beta\text{-}B\alpha)_{inter}$	1.8378	2.857	−0.0063	0.0656	2.50E−3
	1.9756	0.939			2.62E−3
B800	1.8887	2.708	0	0.00085	0
	1.9057	0.974			0
$(A\alpha\text{-}A\beta)_{H-intra}$	1.8239	3.084	−0.0144	0.0804	
	1.9866	0.556			
$(A\beta\text{-}B\alpha)_{H-inter}$	1.8136	2.941	0.0090	0.0671	
	1.9500	0.771			
6-31G*	1.6511	3.177			3.03E−3
$(A\alpha\text{-}A\beta)_{intra}$	1.8384	0.651	−0.0009	0.09043	−6.86E−3
$(A\beta\text{-}B\alpha)_{inter}$	1.6884	2.961			3.64E−3
	1.8306	0.925	−0.0112	0.06811	−3.46E−3

[a] Intra- and interpolypeptide dimers are denoted by the subscripts intra and inter. The subscript H further denotes the calculations which include the H-bonding and Mg ligands (see text).

energy of the *β*B850 Bchl is calculated to be noticeably lower than that of the αB850 Bchl (i.e., that with a planar structure). It is found that some of this difference is compensated for by the interaction of the His Mg ligand with the αB850, which lowers the excitation energy more than for the *β*B850. It is interesting to note that this His residue red-shifts the spectra of each monomer significantly, whereas the H-bonding ligands (αTrp and αTyr) have a lesser effect. These results are in accord with the conclusions of the site-directed mutagenesis studies;[52] it is seen that the excitation energies of the monomers are red-shifted by the H-bonding ligands. However, a significant role does appear to be played by the His residues as well.

In Table 3 the results of the dimer calculations are shown, including the results of analyses using eqs 5, 6, and orbital overlaps determined using calculated MO densities and eq 14. The form of the MOs (with respect to linear combinations of monomer MOs) is very similar to those reported in ref 41. In terms of the LMOs (cf. ref 47), the ordering from HOMO−1 to LUMO+1 is $-\varphi_2$, $-\varphi_1$, $-\varphi_4$, φ_3. The influence of the H-bonding ligands is evident in the spectral shifts of the dimers. The calculated orbital overlap integrals (HOMO−HOMO and LUMO−LUMO) are larger for the 6-31G* calculations than those done at the 3-21G* level owing to the more flexible treatment of the 2s and 2p orbitals in the larger basis set.

TABLE 4: Couplings[a] (cm^{-1}) Calculated for LH2 According to the Scheme Described in Section 4[a]

dimer	V^{CIS}	V^{Coul}(CIS)	V^{short}	V^{Coul}[b]	*V*	V^{d-d} (*κ*)[c]
3-21G*						
$A\alpha\text{-}A\beta$	695	650	45	270	315	415 (1.74)
$A\beta\text{-}B\alpha$	530	490	40	205	245	335 (1.20)
B800	−70	−70	0	−30	−30	−30 (−1.34)
$(A\alpha\text{-}A\beta)_H$	650	545	105	230	335	395 (1.65)
$(A\beta\text{-}B\alpha)_H$	540	425	115	180	295	320 (1.12)
6-31G*						
$A\alpha\text{-}A\beta$	730	675	55	265	320	415 (1.73)
$A\beta\text{-}B\alpha$	550	490	60	195	255	330 (1.19)

[a] Labeling of the dimers is the same as for Table 3. The dipole−dipole coupling is given together with the orientation factor, *κ*, obtained using the CIS dipole transition moments. Values quoted to nearest 5 cm^{-1}. [b] V^{Coul} has been determined assuming an experimental dipole transition moment of 1.33 e Å (6.39 D). It may be scaled to a revised experimental transition moment (say *m*) by $V^{Coul}(new) = V^{Coul}\ |m|^2/1.33^2$. [c] V^{dd} is determined relative to the Mg centers.

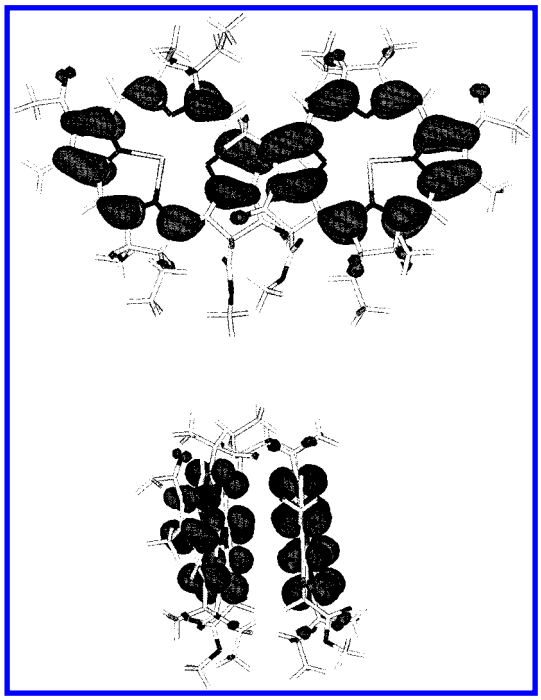

Figure 2. Calculated (HF/6-31G*) HOMO of the intrapolypeptide B850 dimer.

The analysis of the couplings is summarized in Table 4. The HOMO of the intrapolypeptide dimer is depicted in Figure 2. HOMOs for the intra- and interpolypeptide dimers of B850, including the Mg ligands and H-bonding amino acid residues in the calculation, are illustrated in Figure 3. The Coulombic coupling, V^{Coul}, makes the largest contribution to the total couplings. It is found to be insensitive to basis set. The dipole approximation yields identical results to the ab initio results

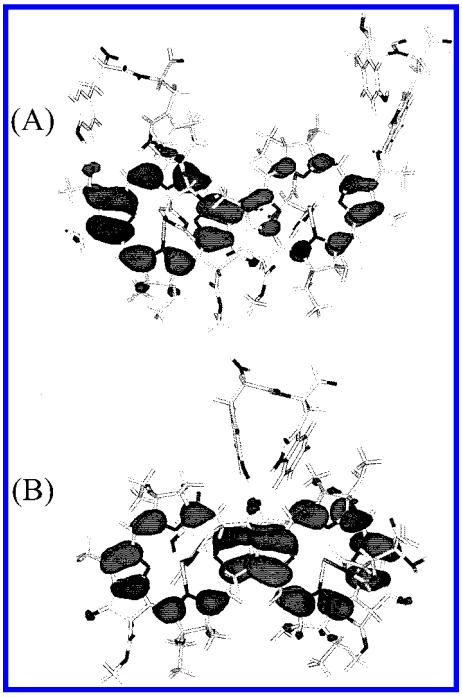

Figure 3. Calculated HOMOs of the B850 dimers. Calculated HOMOs (HF/3-21G*) of the (A) intrapolypeptide and (B) interpolypeptide B850 dimers, including the influence of Mg ligands (His) and H-bonding residues (Trp and Tyr).

for the B800−B800 coupling, demonstrating the reliability of our methodology. As anticipated, the dipole approximation does not reproduce the V^{Coul} for the B850 couplings. Inclusion of the H-bonding ligands in the calculation decreases the calculated Coulombic couplings by about 15%.

The orbital overlap-dependent coupling, V^{short}, is calculated to be similar for both the interpolypeptide dimer and the intrapolypeptide dimer of B850. Inspection of the HOMOs and LUMOs of the dimers leads to the perception that there is more overlapping density in the intrapolypeptide dimer (as suggested by McDermott et al.[1]). However, calculation of the overlaps reveals that there is actually slightly less overlap between monomer HOMOs for the intrapolypeptide dimer owing to the nodal structure of the orbitals, and hence resultant interference effects (Figures 4 and 5). Increasing the basis set from 3-21G* to 6-31G* results in an increase in both the calculated V^{short} and the overlap integrals, as expected. The results obtained using each basis set are similar, leading us to conclude that the 3-21G* basis set is reliable for these calculations. The V^{short} couplings are increased by approximately 30% in going from the 3-21G* to the 6-31G* basis set. We conclude that the orbital overlap-dependent contribution to the coupling for both the intra- and interpolypeptide dimers is at least 60 cm^{-1}. This represents approximately 20% of the total coupling

6. Discussion

The small B800−B800 coupling (in excellent agreement with V^{d-d}) is consistent with an incoherent hopping (i.e., Förster[30]) model for intraband energy transfer.[69] However, it is thought that for B850 that the couplings are of the same magnitude as the disorder (inhomogeneous broadening) and the homogeneous line width. Hence a simple Förster model should be inapplicable. In previous work the energy migration in B850 has been modeled as a hopping between dimers.[12] In that work it was found that the fluorescence depolarization kinetics could be modeled by assuming an intrapolypeptide coupling of 230 cm^{-1}, an interpolypeptide coupling of 110 cm^{-1}, and a site disorder of 200 cm^{-1}. It was suggested that the resultant dynamics could be described as incoherent hopping between dimers[12,15] (prompted by the strong interactions evident in the B820 dimeric subunit of LH1[48−51,70]); however, the authors emphasized that electronic structure calculations were necessary to confirm some the speculation. Pullerits et al.[22] have simulated femtosecond transient absorption experiments of the B850 region after excitation of the B800 band and subsequent energy transfer to B850. Their results suggest a delocalization length of 4 ± 2 molecules. Studies and simulations of superradiance have led Monshouwer et al.[14] to conclude that the delocalization length is approximately 2−3 molecules. Kennis et al.[23] have employed femtosecond transient absorption measurements to compare B850 with the special pair of the reaction center, and conclude that the delocalization length in B850 is 2.5 molecules at 5 K. A key parameter in each of the analyses reported in these studies

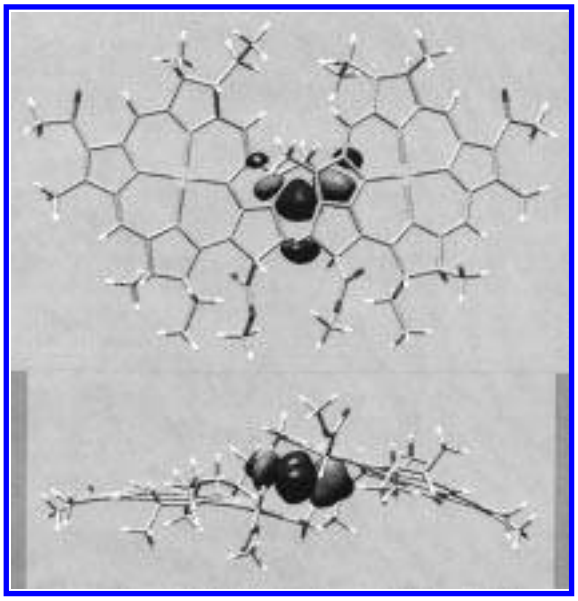

Figure 4. Depiction of the overlap density (HF/3-21G*) between Bchl *a* monomer HOMOs which comprise the intrapolypeptide dimer.

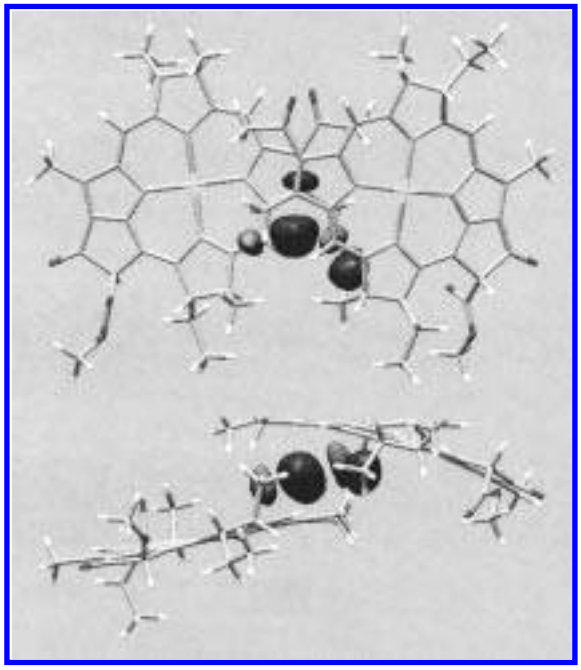

Figure 5. Depiction of the overlap density (HF/3-21G*) between Bchl *a* monomer HOMOs which comprise the interpolypeptide dimer.

is the electronic coupling. Mukamel and co-workers have recently described a method of analysis based on the density matrix, which requires input of disorder, site spectral densities, geometry of the aggregate, and electronic couplings.[24]

Couplings. It is evident from Table 4 that the contribution to the couplings from orbital overlap-dependent interactions (short-range coupling, V^{short}) is relatively small compared to V^{Coul}, in accord with the conclusions of Alden et al.[26] (who did not, however, quantify V^{short}). This is expected for strongly allowed electronic transitions.[35] Similar short-range couplings contribute to both the interpolypeptide coupling and to the intrapolypeptide coupling. We conclude that the orbital overlap-dependent contribution to the coupling for both the intra- and interpolypeptide dimers is at least 60 cm^{-1}. To put this in perspective, it is at least twice the magnitude of the B800−B800 coupling.

It is seen that the dipole approximation significantly overestimates the B850 nearest-neighbor couplings (as shown previously by Krueger et al.[29]). Novoderezhkin and co-workers[23] use the dipole approximation, but find the intra- and interpolypeptide couplings to be 785 and 566 cm^{-1}, respectively, considerably larger even than our V^{d-d} results. This difference is due to their choice of dipole transition moment of 1.61 e Å (cf. our 1.33 e Å) and center-to-center separations of 9.7 and 8.7 Å (rather than 9.53 and 9.05 Å). (It is noted that the center-to-center separations of the B850 Bchls were reported incorrectly in ref 1. The correct distances, which we use here, are obtained from the deposited crystal structure coordinates.)

The results we have obtained for the B850 couplings (in the absence of H-bonding amino acid residues) are similar to those determined by Alden et al.[26] using the QCFF/PI Hamiltonian. The difference in magnitudes of the couplings arises mainly from the different scalings used; we took the Bchl a transition moment to be 1.33 e Å, and they used 1.47 e Å. The results of Sauer et al.,[25] who determined couplings using the monopole approximation, do not reflect the alternation of the intra- and interpolypeptide couplings determined by our calculations. The magnitudes of the couplings suggested by Hu et al.[27] for *Rs. molischianum* (determined by spectral fitting) are significantly different from the ab initio results. We suggest that this may be due, in part, to neglect of the influence of V^{short} on the energies of the exciton states (i.e., approximately via the U of eq 5). This is discussed in ref 47 (cf. eq 13) and in ref 35 (cf. Figure 6 of ref 35a). Neglect of the alternating α/β monomer excitation energies (i.e., Δ of eq 5) would also have influenced the analysis reported in ref 27.

The monomer calculations clearly show an alternation of the excitation energies of the Bchl *a* monomers in B850 such that β-B850 is red-shifted relative to α-B850. This is a result of the marked geometrical differences between the two molecules, as has been established previously,[72] and is discussed by Prince et al.[53] Such an alternation in monomer excitation energies was found to be important for modeling the CD spectra of B850.[73] Modeling the absorption and CD spectra of a B800-free mutant of LH2 (*Rb. sphaeroides*) by Koolhaas et al.[74] suggests that there is an alternation of the monomer energies (803 and 823 nm) and couplings of 300 and 233 cm^{-1}. This is in remarkably close agreement with the results reported in the present work.

H-Bonding Interactions. It has been demonstrated by site-directed mutagenesis in the α subunit of the LH2 complex of *Rb. sphaeroides* that a significant contribution to the red shift of the absorption spectrum of B850 arises from interactions with H-bonding amino acid residues.[52] It was found that single (αTyr44, αTyr45 → PheTyr) and double (αTyr44, αTyr45 → PheLeu) site-specific mutations produced blue shifts of 11 and 24 nm, respectively (at 77 K), of the B850 absorption band. It has also been reported that changing the charged residue βLys23 → Gln produces an 18 nm blue shift in the B850 absorption maximum.[75] A similar situation has been found for the B800 absorption band.[76] Hence it is clear that specific interactions between the Bchls and certain residues play an important role in tuning the absorption spectra, and therefore, for example, the rate of B800 to B850 energy transfer via the resultant effect on the spectral overlap integral.[77]

Some initial calculations which investigate the relationship between structure and red shift of the spectrum have been reported by Sturgis and Robert.[78] Questions which we wish to address in the present work are as follows: (i) Do the H-bonding interactions influence the α/β site energies to different extents? This would affect the delocalization length, and could provide a basis for species-to-species differences. In this regard, the presence and type of carotenoid may also be a factor.[79] (ii) Are there implications for the electronic couplings? Conceivably there could be: inspection of the structure of LH2 reveals that the key H-bonding interactions occur on the outside of the intrapolypeptide dimer pair, but on the inside of the interpolypeptide dimer pair. Indeed, the HOMO shown in Figure 3A appears to be perturbed from that shown in Figure 2 (however, the excited state calculations suggest that this is not a particularly important issue, since the excited states are obtained by linear combinations of several, at least four, different HOMO → LUMO excitations).

The calculations reported in Tables 2 and 3 demonstrate the effect of these specific protein−cofactor interactions on the excitation energies of monomer and dimer Bchl *a* in B850. It is seen from the results collected in Table 2 that the interactions involving the His Mg ligands significantly red-shift the excitation energies of the associated Bchl *a* monomers. The overall ramifications for the B850 absorption band are not immediately clear, since the absorption spectrum reflects the delocalization length of the aggregate. A salient observation, however, is that the excitation energy difference between the α and β B850 monomers (Δ) diminishes from 340 to 265 cm^{-1} when the His residues are included to 200 cm^{-1} when the Trp and Tyr residues are also included. Concomitantly, the excitation energies red-shift primarily via interaction with the His residues. The net effect of decreasing the $\alpha-\beta$ site energy difference is to increase their interaction (assuming the coupling, V, does not change, then for identical chromophores the interaction is V; for a large value of Δ the interaction is approximately V/Δ). The results of the dimer calculations suggest that a significant effect of the specific interactions which we have investigated is to bring the lower dimer exciton bands (i.e., those carrying the bulk of the oscillator strength) of the intra- and interpolypeptide dimers into closer resonance: from an excitation energy difference of 280 cm^{-1} to a difference of only 85 cm^{-1}. This is a significant change relative to the magnitude of the electronic couplings.

In Figure 6 we illustrate the absorption spectrum of B850, calculated using the nearest-neighbor couplings determined at the CIS/6-31G* level, the next-to-nearest neighbor couplings reported in ref 29 (determined using the transition density cube, TDC, method based on CIS/3-21G* calculations), and α and β mean site energies reported here (including the H-bonds and Mg ligands, Table 2), but red-shifted to 1.5558 eV (797 nm) and 1.5313 (810 nm). Site disorder is included using the method of Fidder et al.,[80] as has been employed also by others.[12,14,25,26,73,81,82] We added a Gaussian distribution of disorder with standard deviation 170 cm^{-1} (corresponding to a fwhm of

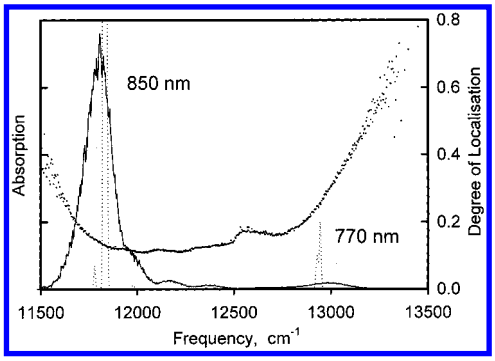

Figure 6. Calculated absorption spectrum of B850. Absorption spectrum of B850, calculated using the nearest-neighbor couplings determined at the CIS/6-31G* level, the next-to-nearest neighbor couplings reported in ref 29 (determined using the transition density cube, TDC, method based on CIS/3-21G* calculations), and α and β mean site energies reported here (including the H-bonds and Mg ligands, Table 2), but red-shifted to 1.5558 eV (797 nm) and 1.5313 (810 nm). The dotted line is the absorption spectrum calculated for negligible site disorder. A Gaussian distribution of disorder with standard deviation 170 cm^{-1} was included in the calculation represented by the solid line (homogeneous line broadening is not included in this simulation). The degree of localization (as defined in ref 78) is also plotted (large dots).

400 cm^{-1}), as determined by Jimenez et al.[13] for the inhomogeneous contribution to the line broadening (i.e., we have not attempted to include homogeneous line broadening in this simulation). The degree of localization (as defined in ref 80) is also plotted and is discussed below. The couplings and $\alpha-\beta$ excitation energy difference which we have calculated clearly reproduce the relative positions and oscillator strengths of the 850 nm band and the upper exciton band, identified recently in a B800-free mutant of *Rb. sphaeroides*.[74]

The total couplings calculated for the B850 dimers with inclusion of the amino acid residues are seen to differ from those from the "dimer only" calculations (Table 4). In fact, they are determined to be larger owing to an increase in V^{short} of approximately 250%. All these calculations were repeated, yielding the same results. However, it is not apparent how the residues could increase the contribution from V^{short}. It is possible that a superexchange mechanism is involved for the case of the interpolypeptide dimer owing to the direct connection of the Trp and Tyr H-bonding residues; however, it is unlikely that orbital overlap-dependent interactions would be mediated through this pathway more efficiently than via the direct orbital overlap. We cannot arrive at any firm conclusions with the available information. In order to obtain a self-consistent picture of how the H-bonding residues perturb the MOs of the Bchls (i.e., to explain the apparent inconsistencies in the dimer orbitals shown in Figure 3) we may need to consider the origin of the electronic transition in terms of linear combinations of single excitations more carefully, for example an "effective hole"−"effective electron" picture.

The decrease in the Coulombic couplings calculated for the B850 dimers (Table 4) when the amino acid residues are included in the calculations is somewhat surprising. It is possible that this comes about because we have neglected the difference in polarization contributions to the couplings in the monomer calculations (they are included at the HF level in the dimer calculations). Alternatively, we could be treating the polarization of each Bchl by the amino acids to different extents in the monomer and the dimer calculations because of partial screening effects owing to the presence of the second monomer. Such effects would possibly be more significant in the presence of the amino acid residues (in other words, we would expect the amino residues to distort the electron densities of the Bchl molecules). Furthermore, the decrease in the Coulombic couplings is presaged by a decrease in orientation factors for the dipole−dipole interactions, which is indicative of microscopic third-body mediation of the Coulombic coupling,[83] since in the limit of an intervening and surrounding dielectric continuum, this tends to a dielectric screening,[84−86] but in the present case may reflect a more specific polarization effect. If this effect is large, we expect our method of calculation to become inaccurate, although further work is required to determine the significance of this correction. In view of this, in our discussions of the spectroscopy of LH2 given below, we refer to the couplings determined in the absence of the H-bonding amino acid residues.

Superradiance. Superradiant fluorescence emission (i.e., enhanced radiative rates of a molecular aggregate compared to a monomer[87]) have been studied recently in LH2 and LH1 (of *Rb. sphaeroides*). An enhancement of the radiative rate of B850 of 2.8 times that of monomeric Bchl *a* at room temperature was reported. Recently, it has been demonstrated using time-correlated single photon counting measurements, time-resolved microwave conductivity measurements, and ab initio MO calculations that radiative rates in molecular dimers can be further increased (i.e., in addition to that expected from the relationship for identical chromophores A and B, $k_{rad(dimer)} \propto |\mu_{A(mon)} \pm \mu_{B(mon)}|^2/2$) by the involvement of short-range contributions to the electronic coupling.[88,89] We find from the calculations reported in the present study, however, that the superradiance electronic enhancement factors for the intra- and interpolypeptide dimers, $K = k_{rad}^{dimer}/k_{rad}^{monomer} = f^{dimer}/f^{monomer}$, are approximately 2.1 and 1.9, respectively (assuming an average monomer oscillator strength of 0.7). If we consider a simple description of the superradiance enhancement factor derived from the relative orientations of monomer transition moments, we find *K* to be 2.0 and 1.9, respectively. Since these values are very similar to those determined by the dimer MO calculations, it is probable that there is only a relatively small contribution to the superradient rate from short-range interactions. In light of the results reported by Monshouwer et al.,[14] we conclude that to rationalize the measured value of *K*, the delocalization length for B850 must therefore be greater than two Bchl *a* molecules, but certainly not greater than the five or six suggested by the degree of localization plotted in Figure 6. (N.B Recall that the simulation shown in Figure 6 does not include contributions from homogeneous line broadening mechanisms, which will increase the degree of localization.) This is in accord with the analysis of Monshouwer et al.[14] (they suggest 3−4 pigments at room temperature).

The negligible temperature dependence of *K* reported by Monshouwer et al.[14] is interesting and suggests that site disorder provides the dominant contribution to line broadening in B850. Possible origins of this disorder have been examined by Papiz and Prince[90] using group anisotropic thermal parameter refinement of the *Rps. acidophila* LH2 crystal structure. They note that the largest principal axes of the transmembrane helix backbone atoms seem to be optimally arranged to apply (slow time scale) vibrational modes into the B850 rings. Hole burning studies of LH2 in *Rb. sphaeroides*[91,92] and *Rps. acidophila*[93] have been reported which address the issue of "homogeneous" versus inhomogeneous line widths.[94] Simulation of three-pulse echo peak shift data and absorption spectra for B850 (*Rb. sphaeroides*) suggest that the homogeneous line width is 188 cm^{-1} fwhm and that of the inhomogeneous line width is 390 cm^{-1} fwhm.[13]

Analysis of Three-Pulse Echo Peak Shift Measurements of B850. As discussed quite some time ago, the rate of energy transfer is critically dependent on the relative magnitudes of the electronic coupling, V, and the homogeneous/inhomogeneous line widths,[30,95,96] Γ (which determine the dephasing time scales). Förster theory[30] can be applied to predict the rate of energy transfer when the condition $V \ll \Gamma$ holds (i.e., when the Fermi Golden Rule applies). It is clear from our results that this is certainly not the case for B850, or even for the coupling between B850 dimers (which is roughly half the coupling between monomers). The elucidation of the energy transfer dynamics is a complex problem, as previously discussed.[12,13,17,24,82,97,98] As emphasized by Kumble and Hochstrasser,[82] careful consideration of the nature of the initial state and the dynamics of its evolution are crucial for the interpretation of results from femtosecond laser measurements. The electronic couplings which we report in the present work are an important parameter required for the detailed modeling of such experimental data.

Mukamel and co-workers[24] have developed the detailed theory necessary to elucidate the meaning of molecular aggregate echo signals, given input of sufficient structural information. Now that we have calculated the electronic couplings in LH2, we are in a position where can begin to calculate the dynamics of energy transfer, and simulate our three-pulse stimulated echo peak shift (3PEPS) data. However, as shown by Mukamel and co-workers,[24] this is complicated owing to the multiple electronic states in resonance with the excitation pulses. Population redistribution amongst these levels occurs during the population period (energy transfer) and many-body effects contribute to dephasing during the coherence periods. Moreover, at times less than approximately 150 fs, there are significant contributions to the 3PEPS signal from ground-state bleaching terms and coherent contributions involving the aggregate two-exciton electronic states. In this regard, we can make some brief comments regarding the incorporation of two-exciton states into a model for B850 dynamics. If orbital overlap-dependent interactions are strong, then the one-exciton states shift relative to the ground state and the two-exciton states (the two-exciton states and the ground state shift to a much lesser extent).[37] In such a case, the difference between the ground to one-exciton transitions and the one- to two-exciton transitions may not be in close accord with the predictions of a Frenkel Hamiltonian.

7. Conclusions

We have suggested a scheme for the ab initio calculation of the electronic coupling in molecular dimers, as well as its delineation into contributions from Coulombic and short range (i.e., that which depends explicitly on interchromophore orbital overlap) couplings. The utility of this methodology was demonstrated by application to the light-harvesting 2 (LH2) complex of the purple photosynthetic bacterium *Rps. acidophila*.

In addition to studying the B800 and B850 Bchl *a* molecules, we have investigated the influence of residues αTyr44 and αTrp45 which form H-bonds from the adjacent α protein to the C3-acetyl group of B850 Bchl *a*, and have been implicated in the spectral shift of the B850 band. Furthermore, we have included in these "H-bond" calculations the His residues which coordinate to the central Mg of each Bchl *a*. The spectral shifts observed in studies using site-directed mutagenesis were reproduced by the calculations. It was found that the large red shift of the excitation energies of monomeric Bchl *a* is caused by the effect of these His Mg ligands. The electronic couplings in B850 were found not to be significantly affected by these H-bonding amino acid residues, despite apparent perturbations of the dimer molecular orbitals.

The Coulombic coupling, V^{Coul}, was found to provide the largest contribution to the total coupling in all cases, and was found to be insensitive to basis set. The dipole approximation yielded identical results to the ab initio results for the B800−B800 coupling, -30 cm^{-1}. As anticipated, the dipole approximation did not reproduce the V^{Coul} for the B850 couplings. Total couplings were determined to be (6-31G* basis set) 320 and 255 cm^{-1} for the intra- and interpolypeptide dimers, respectively, for which contributions from V^{Coul} were found to be 265 and 195 cm^{-1} respectively (using the TDC method).

It was found that couplings from orbital overlap-dependent interactions (short-range coupling, V^{short}) are small, but not insignificant, compared to V^{Coul}. Similar short-range couplings contribute to both the interpolypeptide coupling and to the intrapolypeptide coupling. We found the orbital overlap-dependent contribution to the coupling for both the intra- and interpolypeptide dimers is at least 60 cm^{-1}. This represents approximately 20% of the total coupling. These values were found to be consistent with the magnitude of the interchromophore orbital overlap integrals.

The superradiance electronic enhancement factors for the intra- and interpolypeptide dimers, $K = k_{\mathrm{rad}}^{\mathrm{dimer}}/k_{\mathrm{rad}}^{\mathrm{monomer}} = f^{\mathrm{dimer}}/f^{\mathrm{monomer}}$, were calculated to be ca. 2.1 and 1.9, respectively. In light of the results reported by Monshouwer et al.,[14] we conclude that to rationalize the measured value of K, the delocalization length for B850 must be at least two, but probably no greater than four Bchl *a* molecules.

Acknowledgment. This work was supported by the National Science Foundation. I.R.G. acknowledges the support of the EPSRC through provision of computing resources GR/K 83878. R.J.C. thanks the BBSRC for financial support. Dr Gerry McDermott is acknowledged for helpful discussions. We thank Prof. Mike Zerner for kindly providing us with a preprint of ref 28. NERSC is gratefully acknowledged for provision of computational resources. In particular, we thank Jonathan Carter for assistance in optimizing some of our code.

References and Notes

(1) McDermott, G.; Prince, S. M.; Freer, A. A.; Hawthornthwaite-Lawless, A. M.; Papiz, M. Z.; Cogdell, R. J.; Isaacs, N. W. *Nature* **1995**, *374*, 517.

(2) Kühlbrandt, W.; Wang, D. N.; Fujiyoshi, Y. *Nature* **1994**, *367*, 614.

(3) Karrasch, S.; Bullough, P. A.; Ghosh, R. *EMBO J.* **1995**, *14*, 631.

(4) Koepke, J.; Hu, X.; Muenke, C.; Schulten, K.; Michel, H. *Structure* **1996**, *4*, 581.

(5) Kühlbrandt, W. *Structure* **1995**, *3*, 521.

(6) van Grondelle, R.; Dekker: J. P.; Gillbro, T.; Sundström, V. *Biochim. Biophys. Acta* **1994**, *1187*, 1.

(7) Fleming, G. R.; van Grondelle, R. *Curr. Opinion Struct. Biol.* **1997**, *7*, 738.

(8) Pullerits, T.; Sundström, V. *Acc. Chem. Res.* **1996**, *29*, 381.

(9) Fleming, G. R.; Martin, J.-L.; Breton, J. *Nature* **1988**, *333*, 190.

(10) Yu, J.-Y.; Nagasawa, Y.; vanGrondelle, R.; Fleming, G. R. *Chem. Phys. Lett.* **1997**, *280*, 404.

(11) Bradforth, S. E.; Jimenez, R.; van Mourik, F.; van Grondelle, R.; Fleming, G. R. *J. Phys. Chem.* **1995**, *99*, 16179.

(12) Jimenez, R.; Dikshit, S. N.; Bradforth, S. E.; Fleming, G. R. *J. Phys. Chem.* **1996**, *100*, 6825.

(13) Jimenez, R.; van Mourik, F.; Yu, J. Y.; Fleming, G. R. *J. Phys. Chem. B* **1997**, *101*, 7350.

(14) Monshouwer, R.; Abrahamsson, M.; van Mourik, F.; van Grondelle, R. *J. Phys. Chem. B* **1997**, *101*, 7241.

(15) Visser, H. M.; Somsen, O. J. G.; van Mourik, F.; Lin, S.; van Stokkum, I.; van Grondelle, R. *Biophys. J.* **1995**, *69*, 1083.

(16) Chachisvilis, M.; Pullerits, T.; Jones, M. R.; Hunter, C. N.; Sundström, V. *Chem. Phys. Lett.* **1994**, *224*, 345.

(17) Chachisvilis, M.; Kühn, O.; Pullerits, T.; Sundström, V. *J. Phys. Chem. B* **1997**, *101*, 7275.
(18) Freer, A.; Prince, S.; Sauer, K.; Papiz, M.; Hawthornthwaite-Lawless, A.; McDermott, G.; Cogdell, R.; Isaacs, N. *Structure* **1996**, *4*, 449.
(19) Meier, T.; Chernyak, V.; Mukamel, S. *J. Phys. Chem. B* **1997**, *101*, 2332.
(20) Meier, T.; Zhao, Y.; Chernyak, V.; Mukamel, S. *J. Chem. Phys.* **1997**, *107*, 3876.
(21) Novoderezhkin, V. I.; Razjivin, A. P. *FEBS Lett.* **1995**, *368*, 370.
(22) (a) Zhang, W. M.; Meier, T.; Chernyak, V.; Mukamel, S. *J. Chem. Phys.* **1998**, *108*, 7763. (b) Zhang, W. M.; Meier, T.; Chernyak, V.; Mukamel, S. *Philos. Trans. R. Soc. London, Ser. A* **1998**, *356*, 405.
(23) Pullerits, T.; Chachisvilis, M.; Sundström, V. *J. Phys. Chem.* **1996**, *100*, 10787.
(24) Kennis, J. T. M.; Streltsov, A. M.; Permentier, H.; Aartsma, T. J.; Amesz, J. *J. Phys. Chem. B* **1997**, *101*, 8369.
(25) Sauer, K.; Cogdell, R. J.; Prince, S. M.; Freer, A.; Isaacs, N. W.; Scheer, H. *Photochem. Photobiol.* **1996**, *64*, 564.
(26) Alden, R. G.; Johnson, E.; Nagarajan, V.; Parson, W. W.; Law, C. J.; Cogdell, R. G. *J. Phys. Chem. B* **1997**, *101*, 4667.
(27) (a) Hu, X.; Ritz, T.; Damjanovic, A.; Schulten, K. *J. Phys. Chem. B.* **1997**, *101*, 3854. (b) Hu, X.; Damjanovic, A.; Ritz, T.; Schulten, K. *Proc. Natl. Acad. Sci. U.S.A.* **1998**, *95*, 5935.
(28) Zerner, M. C.; Cory, M. G.; Hu, X.; Schulten, K., submitted for publication.
(29) (a) Krueger, B. P.; Scholes, G. D.; Fleming, G. R. *J. Phys. Chem. B* **1998**, *102*, 5378. (b) Krueger, B. P.; Scholes, G. D.; Fleming, G. R. *J. Phys. Chem. B* **1998**, *102*, 9603.
(30) (a) Förster, Th. *Ann. Phys.* **1948**, *2*, 55. (b) Förster, Th. Delocalized Excitation and Excitation Transfer. In *Modern Quantum Chemistry*; Academic Press: New York, 1965; Vol. III.; p 93.
(31) Scholes, G. D.; Andrews, D. L. *J. Chem. Phys.* **1997**, *107*, 5374.
(32) Scholes, G. D. and Ghiggino, K. P. *J. Phys. Chem.* **1994**, *98*, 4580. Note the following corrections in eqs 7: eq 7e replace $(ab|ab')$ with $(ab|a'b')$, eq 7f replace $2(a'|a)t$ with $(a'|a')t$, and eq 7g replace $3(aa|bb)q + (aa|a'b')$ with $2(aa|bb)q + 3(aa|a'b')$.
(33) Andrews, D. L. *Chem. Phys.* **1989**, *135*, 195.
(34) Harcourt, R. D.; Scholes, G. D.; Ghiggino, K. P. *J. Chem. Phys.* **1994**, *101*, 10521.
(35) Scholes, G. D.; Harcourt, R. D.; Ghiggino, K. P. *J. Chem. Phys.* **1995**, *102*, 9574.
(36) Dexter, D. L., *J. Chem. Phys*. **1953**, *21*, 836.
(37) (a) Scholes, G. D. *J. Phys. Chem.* **1996**, *100*, 18731. (b) Scholes, G. D. and Ghiggino, K. P. In *Advances in Multiphoton Processes and Spectroscopy*; Lin, S. H., Villaeys, A. A.; Fujimura, Y. Eds.; World Scientific: Singapore, 1998; pp 95−331 Vol. 10.
(38) Kouteck, J.; Paldus, J. *Theor. Chim. Acta (Berlin)* **1963**, *1*, 268.
(39) Kouteck, J.; Paldus, J. *Collect. Czech. Chem. Commun*. **1962**, *27*, 599.
(40) Polák, R.; Paldus, J. *Theor. Chim. Acta (Berlin)* **1966**, *4*, 37.
(41) Thompson, M. A.; Zerner, M. C.; Fajer, J. *J. Phys. Chem.* **1990**, *94*, 3820.
(42) Warshel, A.; Parson, W. W. *J. Am. Chem. Soc.* **1987**, *109*, 6143.
(43) (a) McGlynn, S. P.; Armstrong, A. T.; Azumi, T. In *Modern Quantum Chemistry*; Sinanoglu, O., Ed.; Academic Press: New York, 1965; Vol. 3. (b) Azumi, T. and McGlynn, S. P. *J. Chem. Phys.* **1965**, *42*, 1675.
(44) Murrell, J. N.; Tanaka, J. *Mol. Phys.* **1964**, *7*, 363.
(45) McWeeny, R. *Methods of Molecular Quantum Mechanics*, 2nd ed.; Academic Press: London, 1992.
(46) Scholes, G. D.; Harcourt, R. D. *J. Chem. Phys.* **1996**, *104*, 5054.
(47) Scholes, G. D.; Harcourt, R. D.; Fleming, G. R. *J. Phys. Chem. B* **1997**, *101*, 7302.
(48) (a) Zuber, H. *Photochem. Photobiol.* **1985**, *42*, 821. (b) Bunisholz, R. A.; Zuber, H. *J. Photochem. Photobiol. B* **1992**,*15*, 113.
(49) Braun, P.;. Scherz, A. *Biochemistry* **1991**, *30*, 5177.
(50) Parkes-Loach, P. S.; Sprinkle, J. R.; Loach, P. A. *Biochemistry* **1988**, *27*, 7, 2718.
(51) (a) Meadows, K. A.; Parkes-Loach, P. S.; Kehoe, J. W.; Loach, P. A. *Biochemistry*, **1998**, *37*, 3411. (b) Kehoe, J. W.; Meadows, K. A.; Parkes-Loach, P. S.; Loach, P. A. *Biochemistry*, **1998**, *37*, 3418.
(52) Fowler, G. J. S.; Visschers, R. W.; Grief, G. G.; van Grondelle, R.; Hunter, C. N. *Nature* **1992**, *355*, 848.
(53) Prince, S. M.; Papiz, M. Z.; Freer, A. A.; McDermott, G.; Hawthornthwaite-Lawless, A. M.; Cogdell, R. J.; Isaacs, N. W. *J. Mol. Biol.* **1997**, *268*, 412.
(54) McCluskey; Prine; Isaacs; Cogdell. Unpublished results.
(55) Robert, B.; Lutz, M. *Biophys. Biochim. Acta* **1985**, *807*, 10.
(56) *Gaussian 94*; Frisch, M. J., Head-Gordon, M., Trucks, G. W., Foresman, J. B., Schlegel, H. B., Ragavachari, K., Robb, M., Binkley, J. S., Gonzalez, C., DeFrees, D. J., Fox, D. J., Whiteside, R. A., Seeger, R., Melius, C. F., Baker, J., Martin, R. L., Kahn, L. R., Stewart, J. J. P., Topiol, S., Pople, J. A., Gaussian, Inc.: Pittsburgh, PA, 1994.
(57) Foresman, J. B.; Head-Gordon, M.; Pople, J. A.; Frisch, M. J. *J. Phys. Chem.* **1992**, *96*, 135.
(58) Hariharan, P. C.; Pople, J. A. *Theor. Chim. Acta* **1973**, *28*, 213.
(59) Thompson, M. A.; Zerner, M. C. *J. Am. Chem. Soc.* **1991**, *113*, 8210.
(60) Warshel, A. and Parson, W. W., *J. Am. Chem. Soc.* **1987**, *109*, 6152.
(61) Pople, J. A.; Segal, G. A. *J. Chem. Phys.* **1965**, *43*, S136.
(62) Pople, J. A.; Beverige, D. L.; Dobash, P. A. *J. Chem. Phys.* **1967**, *47*, 2026.
(63) Warshel, A.; Karplus, M. *J. Am. Chem. Soc.* **1972**, *94*, 5612.
(64) Ridley, J.; Zerner, M. *Theor. Chim. Acta* **1973**, *32*, 111.
(65) Mulliken, R. S.; Rieke, C. A.; Orloff, H. *J. Chem. Phys.* **1949**, *17*, 1248.
(66) Scholes, G. D.; Ghiggino, K. P.; Wilson, G. J. *Chem. Phys.* **1991**, *155*, 127.
(67) Warshel, A.; Huler, E. *Chem. Phys.* **1974**, *6*, 463.
(68) (a) Matos, J. M. O., Roos, B. O. and Malmqvist, P.-A. *J. Chem. Phys.* **1987**, *86*, 1458. (b) Matos, J. M. O. and Roos, B. O. *Theor. Chim. Acta* **1988**, *74*, 363. (c) Serrano-Andres, L.; Merchan, M.; Rubio, M.; Roos, B. O. *Chem. Phys. Lett.* **1998**, *295*, 195. (d) Pierloot, K.; De Kerpel, J. O. A.; Ryde, U.; Roos, B. O. *J. Am. Chem. Soc.* **1997**, *119*, 218. (e) Rauk, A.; Yu, D.; Borowski, P.; Roos, B. *Chem. Phys.* **1995**, *197*, 73.
(69) Hess, S.; Åkesson, E.; Cogdell, R. J.; Pullerits, T.; Sundström, V. *Biophys. J.* **1995**, *69*, 2211.
(70) Bradforth, S. E.; Jimenez, R.; van Mourik, F.; van Grondelle, R.; Fleming, G. R. *J. Phys. Chem.* **1995**, *99*, 16179.
(71) (a) Novoderezhkin, V. I.; Razjivin, A. P. *Biophys. J.* **1995**, *68*, 1089. (b) Dracheva, T. V.; Novoderezhkin, V. I.; Razjivin, A. P. *Photosynth. Res.* **1996**, *49*, 269.
(72) Gudowska-Nowak, E.; Newton, M. D.; Fajer, J. *J. Phys. Chem.* **1990**, *94*, 5795.
(73) Koolhaas, M. H. C.; van der Zwan, G.; Frese, R. N.; van Grondelle, R. *J. Phys. Chem. B* **1997**, *101*, 7262.
(74) Koolhaas, M. H. C.; Frese, R. N.; Fowler, G. J. S.; Bibby, T. S.; Georgakopoulou, S.; van der Zwan, G.; Hunter, C. N.; van Grondelle, R. *Biochemistry* **1998**, *37*, 4693.
(75) Fowler, G. J. S.; Crielaard, W.; Visschers, R. W.; van Grondelle, R.; Hunter, C. N. *Photochem. Photobiol.* **1993**, *57*, 2.
(76) Gall, A.; Fowler, G. J. S.; Hunter, C. N.; Robert, B. *Biochemistry* **1997**, *36*, 16282.
(77) Hess, S.; Visscher, K. J.; Pullerits, T.; Sundström, V. *Biochemistry* **1994**, *33*, 8300.
(78) Sturgis, J. N.; Robert, B. *Photosynth. Res.* **1996**, *50*, 5.
(79) Scholes, G. D.; Krueger, B. P.; Gould, I. R.; Fleming, G. R. Unpublished results.
(80) Fidder, H.; Knoester, J.; Wiersma, D. A. *J. Chem. Phys.* **1991**, *95*, 7880.
(81) Durrant, J. R.; Klug, D. R.; Kwa, S. L. S.; van Grondelle, R.; Porter, G.; Dekker: J. P. *Proc. Natl. Acad. Sci. U.S.A.* **1995**, *92*, 4798.
(82) Kumble, R.; Hochstrasser, R. M. *J. Chem. Phys.* **1998**, *109*, 855.
(83) Craig, D. P.; Thirunamachandran, T. *Chem. Phys.* **1989**, *135*, 37.
(84) Juzeliunas, G.; Andrews, D. L. *Phys. Rev. B* **1994**, *49*, 8751.
(85) Dow, J. D. *Phys. Rev.* **1968**, *174*, 962.
(86) Moog, R. S.; Kuki, A.; Fayer, M. D.; Boxer, S. G. *Biochemistry* **1984**, *23*, 1564.
(87) Spano, F. C.; Mukamel, S. *J. Chem. Phys.* **1989**, *91*, 683.
(88) Scholes, G. D.; Turner, G. O.; Ghiggino, K. P.; Paddon-Row: M. N.; Piet, J. J.; Schuddeboom, W.; Warman, J. M. *Chem. Phys. Lett.* **1998**, *292*, 601.
(89) Clayton, A. H. A.; Scholes, G. D.; Ghiggino, K. P.; Paddon-Row: M. N. *J. Phys. Chem.* **1996**, *100*, 10912.
(90) Papiz, M. Z.; Prince, S. M. *Proc. CCP4 Study Weekend* **1996**, 115−123.
(91) Reddy, N. R. S.; Small, G. J. *J. Chem. Phys.* **1991**, *94*, 7545.
(92) Reddy, N. R. S.; Picorel, R.; Small, G. J. *J. Phys. Chem.* **1992**, *96*, 6458.
(93) Wu, H.-M.; Ratsep, M.; Lee, I.-J.; Cogdell, R. J.; Small, G. J. *J. Phys. Chem. B* **1997**, *101*, 7654.
(94) Wu, H.-M.; Small, G. J. *Chem. Phys.* **1997**, *218*, 225.
(95) Simpson, W. T.; Peterson, D. L. *J. Chem. Phys.* **1957**, *26*, 588.
(96) Robinson, G. W.; Frosch, R. P. *J. Chem. Phys.* **1963**, *38*, 1187.
(97) Kühn, O.; Sundström, V. *J. Phys. Chem. B* **1997**, *101*, 3432.
(98) Kühn, O.; Renger, T.; May, V.; Voigt, J.; Pullerits, T. Sundström, V. *Trends Photochem. Photobiol.* **1997**, *4*, 213.